Role of Working Pressure and Deposition Power on the Tribological Performance of TiAlN Thin Films

Kamlesh V. Chauhan *, Sushant Rawal *, Nicky P. Patel, Dattatraya Subhedar, Vandan V. Vyas

Posted Date: 22 May 2026

doi: 10.20944/preprints202605.1513.v1

Keywords: tribology; friction; wear; sputtering; titanium aluminum nitride; thin films

 doi:10.20944/preprints202605.1513.v1

Article

Role of Working Pressure and Deposition Power on the Tribological Performance of TiAlN Thin Films

Kamlesh V. Chauhan [1,*], Sushant Rawal [2,*], Nicky P. Patel [1], Dattatraya Subhedar [1] and Vandan V. Vyas [3]

[1] CHAMOS Matrusanstha Department of Mechanical Engineering, Chandubhai S. Patel Institute of Technology (CSPIT), Charotar University of Science and Technology (CHARUSAT), Changa-388421, Gujarat, India

[2] McMaster Manufacturing Research Institute (MMRI), Department of Mechanical Engineering, McMaster University, 1280 Main Street West, Hamilton, ON L8S4L7, Canada

[3] L.J. Institute of Engineering and Technology, L.J. University, Ahmedabad

* Correspondence: kamleshchauhan.me@charusat.ac.in (K.V.C.); sushant@mcmaster.ca (S.R.)

Abstract

Application of Titanium Aluminium Nitride (TiAlN) coatings on brass surfaces was accomplished using magnetron sputtering. Within the scope of this study, we evaluate the ways in which alterations to the sputtering power and working pressure influence the tribological and structural attributes of TiAlN films. For the purpose of analysing the surface morphology of the TiAlN coating, the scanning electron microscope (SEM) method was utilised. There was a progressive rise in the strength of the TiAlN coating's (103) and (107) peaks in each of the variations. An analysis was conducted to evaluate the tribological properties of the TiAlN coating using a pin-on-disc tribometer. The study involved varying the speeds, loads, and sliding lengths. The wear rates of brass pins coated with TiAlN ranged between 1.03×10^{-3} and 5.87×10^{-4} mm^3/Nm, depending on the load, sliding distance, and speed. Conversely, TiAlN-coated brass pins prepared at varying power showed wear rates ranging from 1.83×10^{-4} to 5.87×10^{-4} mm^3/Nm.

Keywords: tribology; friction; wear; sputtering; titanium aluminum nitride; thin films

1. Introduction

Coating technologies are essential to many parts of our daily life. Modern coatings and films have several potential uses, from consumer apparel and pharmaceuticals to industrial machinery, automobiles and building components [1]. A thin film or coating applied on bulk materials or other surfaces can provide protection, enhance their properties, or impart new functions and attributes. Among these features and functions include the ability to prevent ice, hydrophobicity, and microbiological contamination [2–4]. A major emphasis in modern industrial systems is on developing and fabricating materials with decreased wear characteristics and a coefficient of friction that may be used in a variety of operating applications. The substantial requirement for friction prevention and wear protection in industry has led to a stratospheric rise in coating technology. Innovations in enabling technologies have increased the requirement for innovative coatings with satisfactory mechanical properties and tribological performance.

Several sectors make extensive use of metal nitride coatings made of titanium, namely TiN. These industries include tool production, medical implant, aerospace engineering, and vehicle manufacture. The possible explanation for these coatings' widespread usage is their extraordinary attributes, including outstanding resistance to wear, reduction in friction capabilities, resistance to corrosion, and significant hardness. Several methods are utilised when applying these coatings, such as magnetron sputtering, chemical vapour deposition, and other comparable processes [5–10]. There has been significant research and commercial attention in recent years towards the development of

 doi:10.20944/preprints202605.1513.v1

advanced ternary nitride coatings. The focus on this matter arises from the necessity to improve coating attributes such a higher melting temperature, better resistance to wear and corrosion, and a higher hardness, among other factors. Adding a third element, such as aluminium (Al), molybdenum (Mo), vanadium (V), etc., to titanium nitride (TiN) has been noted that the wear resistance of the resultant films is improved and the friction is reduced [11–13]. The introduction of a small quantity of the third chemical causes changes in the structure, composition, and bonding properties of the film coating [14,15].

The use of titanium aluminium nitride (TiAlN) films has increased because of their many desirable mechanical properties, including their high hardness, resistance to wear, and resistance to corrosion [16]. There are a number of additional benefits to using TiAlN films [17]. TiAlN possesses both a high conductivity coefficient and a low thermal expansion coefficient [18]. Among the many fields that make use of these coatings is the semiconductor device industry, where they prevent damage to semiconductor devices by acting as an electrode barrier [19]. Bioimplant coatings made of TiAlN sheets are another bio application usage [20]. The use of DMLS (direct metal laser sintered) technology to produce titanium implants is a recent development in the field of biomedicine [21]. The medical area is still making use of alloys based on cobalt and nickel, although titanium and its alloys are quickly gaining popularity [22–24].

TiAlN is a ternary nitride coating that provides important technological significance in many different kinds of functions, including high temperature wear resistance due to its high oxidation resistance. Greater chemical stability controls the oxidation resistance of TiAlN, which is superior than coatings established of binary nitrides like AlN and TiN. At room temperature, TiN is present in this material as a rock salt structure with metallic conductivity. On the other hand, at high pressure, AlN can form a metastable rock salt structure after crystallising in a wurtzite structure. TiAlN is the result of Al being incorporated into the face centred cubic (fcc) TiN structure on Ti sites. The hardness, high temperature oxidation resistance, and durability against wear of the TiAlN alloy are all improved by structural refinement. The exceptional hardness of TiN serves as a barrier against wear and tear while sliding. On the other hand, materials with a soft phase such as AlN are advantageous when it comes to achieving a low friction coefficient. Furthermore, the friction and wear characteristics get intricate when many compositions and phases are present within the TiAlN coatings [25].

There is a scarcity of published research that corresponds to the investigation of a number of features of coatings made of titanium aluminium nitride (TiAlN). TiAlN coatings were intended to be developed on brass substrates by the use of the reactive magnetron sputtering process, which was the objective of this investigation. This research initiative is meant to study the impact of pressure as well as change in titanium power on the tribological and structural characteristics of TiAlN coatings. Brass pins are relatively soft and reducing the wear rate of such materials can find its uses in various applications.

2. Materials and Methods

In a cylindrical vessel that was custom-made by Excel Instruments, India, titanium aluminum nitride (TiAlN) films were applied utilizing DC magnetron sputtering. During the sputtering process, a 50.8 mm diameter titanium and aluminium target of 99.99% purity was employed. At first, the cylinder was drained to a pressure of roughly 6×10^{-4} Pa using a turbo molecular pump assisted by a rotary pump. Afterwards, the cylinder was loaded with argon and nitrogen gas with an excellent purity, specifically 99.99%. Gas flow was regulated and maintained at a consistent rate using a mass flow controller (MFC) (ALICAT instruments, USA). For the first set of samples sputtering pressure was adjusted in the range of 1, 1.5, 3, and 5 Pa (sample name AlP1, AlP1.5, AlP3, and AlP5) while target power for titanium and aluminium was maintained at 450 and 275 W respectively, while for the next set of samples titanium power was changed from 275, 350, 400, and 450 W (sample name AlTi275, AlTi350, AlTi400, and AlTi450) while the aluminium power was fixed at 275 W respectively. Target to substrate distance was 50 mm, deposition period was 60 minutes, and substrate

 doi:10.20944/preprints202605.1513.v1

temperature was maintained at 500 °C for all depositions. The N_2:Ar gas ratio, expressed in standard cubic centimetres, was fixed at 08:32.

Utilizing a Bruker X-ray diffractometer (Model D2 Phaser) equipped with Cu-Kα radiation at a wavelength of 1.54 Å, the texture evolution of TiAlN coatings was evaluated. The SEM (Scanning Electron Microscope) was used to analyse the microstructure of the coatings, the model used for this analysis was the EVO-18, manufactured by ZEISS. A pin-on-disc tribometer (Ducom) was used to conduct wear and friction testing under ambient conditions, avoiding the use of lubricant. The experimental setup used in the testing was a pin-on-disc tribological system. The utilized pin was 30 mm in height and 12 mm in diameter; it was constructed of brass (grade 1, IS-3). It came into contact with a disk that was 8 mm in height and 165 mm in circumference. Brass pins, both uncoated and coated with TiAlN, were subjected to a tribological test by rotating on a disc of 60 HRc EN-31 hardened steel (BS 970-1955). The experiment was conducted under ambient conditions. The load values employed were 10, 20, 30, and 40 N, all falling within the acceptable range. During the sliding condition, the length of the course covered ranged from 628 to 785 meters.

3. Results and Discussion

X-ray diffractometer was utilized to assess the changes in texture of TiAlN films. Figure 1(a) illustrates XRD patterns of TiAlN coatings fabricated at various deposition pressures, specifically 1, 1.5, 3, and 5 Pa. It is evident that all of the samples that are coated with TiAlN coating include orientations that are correspondingly (103) and (107). As the deposition pressure decreases from 5 Pa to 1 Pa, the strength of the (103) and (107) peaks improve. At a pressure of 1 Pa, the XRD patterns reveal the existence of orientations (100), (103), and (107). Ait-Djafer et al. (2015) conducted a research where they analyzed the XRD patterns at 40 mTorr. Their findings revealed the existence of TiN with a face-centered cubic (fcc) structure and hexagon AlN patterns. The detection of AlN in a hexagonal crystal structure is only observed under a pressure of 40 mTorr, with a specific orientation of (1 0 0). At a pressure of 30 mTorr, the hexagonal close-packed (hcp) phase of aluminum nitride (AlN) is not present, and only the face-centered cubic (fcc) structure of AlN can be observed. The crystallographic planes obtained were (111), (200), (220), and (311). The TiAlN films have a cubic crystal structure with a (111) orientation at a pressure of 20 mTorr [26].

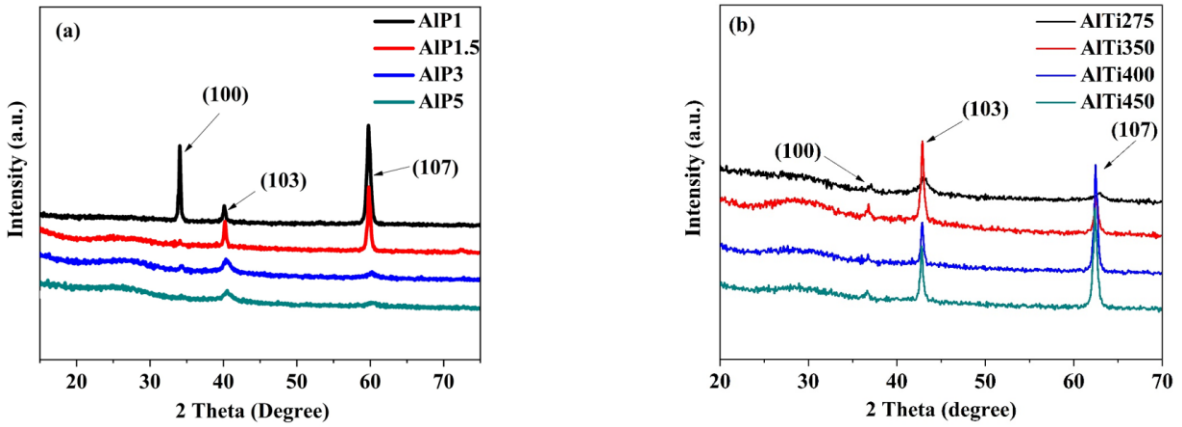

Figure 1. XRD patterns of titanium aluminum nitride (TiAlN) films coated at varied (a) pressure and (b) titanium power.

Figure 1(b) displays the XRD patterns of TiAlN films that were deposited with various titanium power levels of 275, 350, 400, and 450 W. The TiAlN coating exhibits peaks at (100), (103), and (107) across all power variations. When the power is elevated from 275 to 450 W, there is an observed rise in the intensity of the (103) and (107) peaks. The number of atoms expelled and reaching the surface increased as the coating power increased, thus impacting the bombardment of high-energy particles

 doi:10.20944/preprints202605.1513.v1

on the expanding thin layer. These components give the depositing atoms thermal energy, which promotes their mobility on the substrate and, in turn, improves the crystal structure of the coatings that are produced. When the working pressure was adjusted from 1 Pa to 5 Pa, the coating shown a growth orientation preference of (103), as indicated by the X-ray diffraction (XRD) graphs depicted in Figure 1(a).

Additionally, the coating displayed a thick, homogeneous, uniform, and highly compact structure, as observed in the SEM images presented in Figures 2(a) to 2(d). Figures 2(e) to 2(h) depict the morphology of TiAlN films that were developed at different target powers. The SEM images reveal that the TiAlN coatings exhibit a homogeneous, crack-free, and circular surface across all samples. Conventional sputtered (Ti,Al)N coatings typically exhibit a smoother and columnar structure, devoid of macroparticles.

The experiment revealed that size of crystallites in TiAlN coatings reduced from 22 nm to 8 nm when the deposition pressure climbed from 1 to 5 Pa which was studied using Scherrer's equation [27] , as seen in Figure 3(a). Bobzin et. al. (2007) conducted a study on the relationship between hardness and grain size of deposited coatings. Their findings indicate that coatings with smaller crystallite size tend to exhibit higher hardness [28].

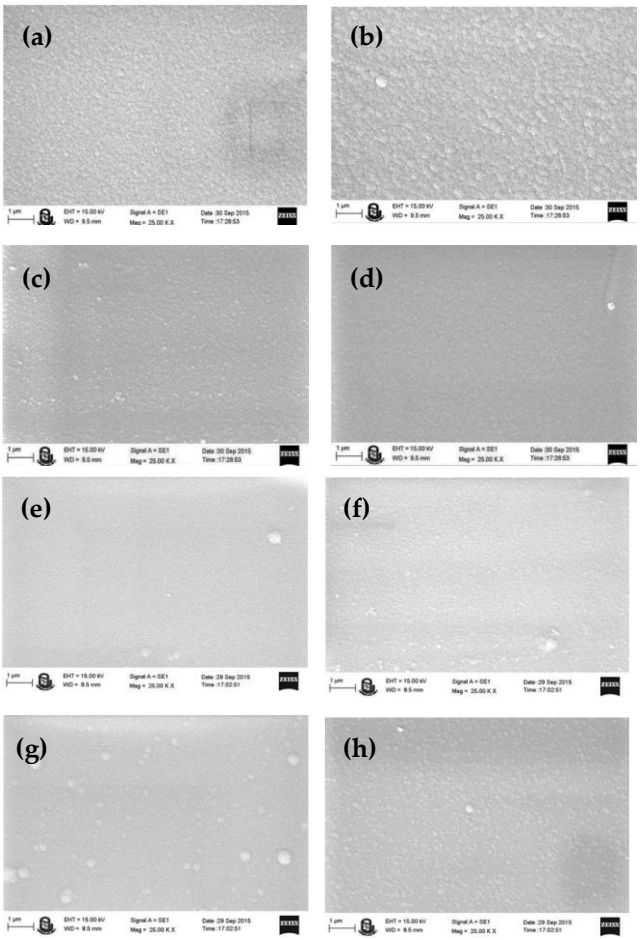

Figure 2. SEM images of TiAlN coatings deposited by various pressures (a) 1, (b) 1.5, (c) 3, and (d) 5 Pa and various power levels (e) 275 W, (f) 300 W, (g) 400 W, and (h) 450 W.

 doi:10.20944/preprints202605.1513.v1

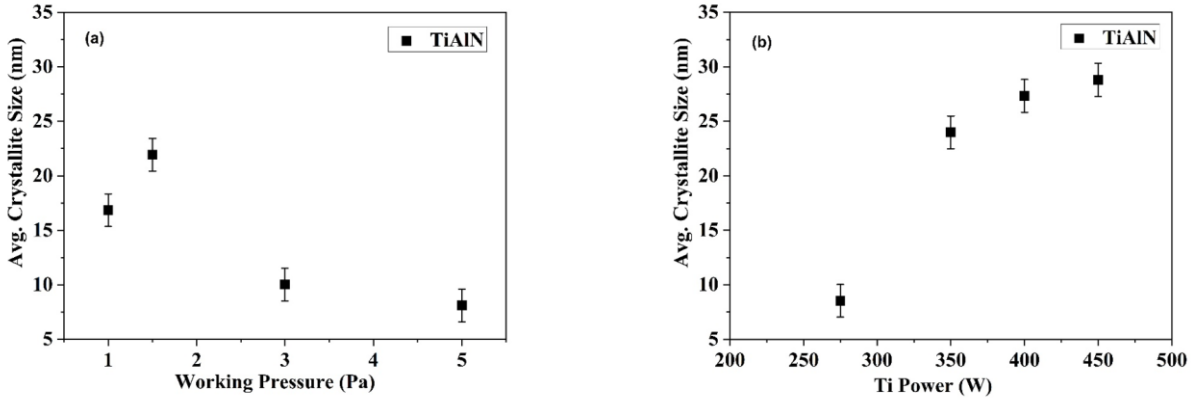

Figure 3. Average crystallite size of titanium aluminum nitride (TiAlN) coatings deposited at different (a) pressure and (b) Titanium power.

The size of the crystallite was determined by the Scherrer equation (1). The formula used to calculate the size was [29]:

$$D = \frac{0.94\lambda}{\Delta\omega cos\theta_B} \quad \text{.....(1)}$$

where θ_B represents Bragg angle, $\Delta\omega$ is the peak's FWHM, λ represents wavelength and D is the average size of crystallite.

The developed coatings' crystallite size improved as the titanium target power was raised. The range of crystallite size as seen in Figure 3(b), exhibits variation between 9 nm and 29 nm. This variation is observed when the target power of titanium is raised from 275 W to 450 W.

The principal aim of tribological research is to foster the development of surface designs that efficiently restrict or control the ratio of friction as well as wear. Empirical evidence has substantiated the existence of a direct proportionality between the force of friction and the load being applied. The coefficient of friction, represented by Equation (2), quantifies this relationship [30].

$$\mu = \frac{F}{W} \quad \text{...(2)}$$

where "μ" for the coefficient of friction (COF), "W" for the applied load, and "F" stands for the frictional force.

Figures 4(a) and 4(b) display the friction coefficients of brass pins, both untreated and coated with TiAlN, at deposition pressures of 1 Pa and 5 Pa, respectively. Figure 4(a) demonstrates a consistent reduction in friction coefficients as the weight increases. Coefficients of friction for the untreated brass pin declined from 0.287 to 0.22 under a load ranging from 10 to 40 N. Depending on the load applied, the friction coefficient of the AlP1 and AlP5 coatings in the sample ranges from 0.195 to 0.24. The coefficient of friction of the AlP1 coating decreased from 0.24 to 0.20 when the load was increased from 10 to 40 N. Similarly, the AlP5 coating reduces the coefficient of friction from 0.23 to 0.19. When exposed to a force of 40 N, the sample AlP5 exhibits a minimum coefficient of friction value of 0.19. The relationship between sliding lengths and the coefficient of friction under a force of 10 N is shown in Figure 4(b). In light of the findings from the experiments, when the sliding distance increases, the coefficients of friction for brass pins that are uncoated and those that are coated with TiAlN show an increasing tendency. As the sliding distance increases, the friction coefficient of an uncoated brass pin goes up from 0.287 to 0.321. Depending on the sliding distance, the friction coefficients of the AlP1 and AlP5 coatings in the sample range from 0.235 to 0.28. Slide distances between 628 and 785 m show an increase in the coefficient of friction for the AlP1 coating sample, from 0.24 to 0.28. Similarly, for sample AlP5 coating, the coefficient of friction increases from 0.235 to 0.265.

 doi:10.20944/preprints202605.1513.v1

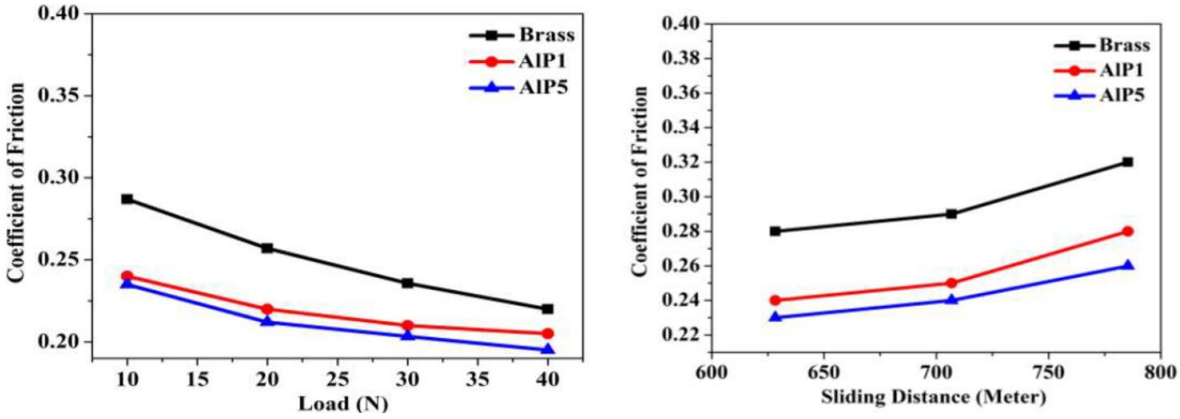

Figure 4. Comparison of uncoated and TiAlN-coated (at various pressure 1 and 5 Pa) brass pins with respect to coefficient of friction (COF) under varying (a) loads and (b) sliding distances.

The sliding distance and load affect the frictional coefficient of untreated and TiAlN-coated brass pins coated at titanium target power of 275 and 450 W, respectively, as illustrated in Figure 5(a) and (b). Coefficients of friction decrease with increasing load, as seen in Figure 5(a). Under a load increase from 10 to 40 N, the uncoated brass friction coefficients dropped from 0.287 to 0.22. The sample's AlTi275 and AlTi450 coatings exhibit a friction coefficient ranging from 0.19 to 0.23 under different loads. The AlTi275-coated sample's coefficient of friction decreased from 0.22 to 0.19 as the load was raised from 10 to 40 N. The coefficient of friction also dropped from 0.23 to 0.19 for the sample with the AlTi450 coating. Under a 10 N load, the correlation between sliding lengths and friction coefficient is shown in Figure 5(b). The friction coefficients of bare and TiAlN-coated brass pins vary with power levels, as seen in the figures, particularly at 275 and 450 W. There is a positive link between the coefficients and the increasing sliding distance. Uncoated brass pins have friction coefficients ranging from 0.287 to 0.321, which rises with increasing sliding distance. Depending on the sliding distance, the sample's AlTi275 and AlTi450 coatings exhibit friction coefficients ranging from 0.20 to 0.26. As the sliding distance is increased from 628 to 785 m, the coefficient of friction for the AlTi275 coating sample goes up from 0.22 to 0.24. The Al-Ti450 coated sample also shows an increase in coefficient of friction, going from 0.23 to 0.26. After the contact time has passed, the TiAlN coating clearly has lower friction coefficients than the exposed brass.

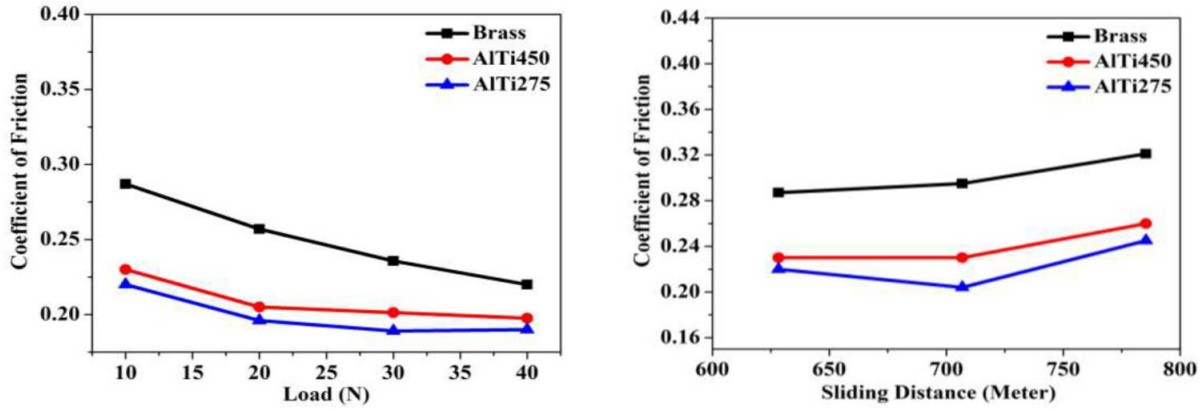

Figure 5. Comparison of uncoated and TiAlN-coated (at various power level at 450 and 275 W) brass pins with respect to coefficient of friction (COF) under varying (a) loads and (b) sliding distances.

The normal load and coefficient of friction are inversely related in the observed range. Because surface roughness increases and wear debris accumulates at a substantial rate, friction decreases as

 doi:10.20944/preprints202605.1513.v1

normal load increases. The friction coefficient exhibits a slight increase as the sliding distance increases. This phenomenon arises from the heat generated at the asperities formed by the sliding contact between two materials. As a result, the temperature increases at the surfaces where friction occurs between these materials, thereby impacting various material properties such as stress, adhesion, and transfer behaviour.

The degree of wear noticed is dependent on several elements, including the surface's hardness, the applied load, and the distance traversed when sliding. The wear volume loss calculation is done using equation (3) as shown below [31]:

$$V = \frac{cLx}{H} \quad \ldots(3)$$

where "x" is the sliding distance, "L" is the load, "H" is the surface hardness, and "c" is a non-dimensional constant.

The rate of wear is determined using Equation (4) shown below [32]:

$$Wear\ rate = \frac{wear \times \pi \times d^2}{4 \times Load \times SD} \frac{mm^3}{Nm} \quad \ldots(4)$$

where "SD" stands for sliding distance and "d" for the pin's diameter.

Figure 6(a) depicts the correlation between the load applied and the rate at which brass pins wear, both untreated and coated with TiAlN, under varying deposition pressures of 1 Pa and 5 Pa. When subjected to the same circumstances of wear, it is evident that the amount of degradation of an untreated brass pin is greater in comparison to that of a TiAlN treated brass pin. Under different loads, the AlP1 and AlP5 coatings, along with the brass pin, experience wear rates ranging from 1.03x10-3 to 5.87x10-4 mm3/Nm. For an uncoated brass pin, increasing the load from 10 N to 40 N causes the wear rate to go from 3.51x10-4 to 5.87x10-4 mm3/Nm. Wear rates for samples coated with AlP1 and AlP5 also rise, from 2.37x10-4 and 5.18x10-4 mm3/Nm and 2.17x10-4 and 5.05x10-4 mm3/Nm, respectively. The graph illustrates that the rate of wear rises in correlation with an increase in the typical load. This phenomenon occurs because when the applied load rises, frictional heat is generated at the site of contact, leading to a loss in the strength of materials. Figure 6(b) depicts the influence of the distance over which the brass pins slide on the rate at which they wear down. This applies to both the pins that are not coated and those that are coated with TiAlN. The specimens utilized for this investigation were AlP1 and AlP5. The uncoated brass pin demonstrates an increase in wear rate from 3.51x10-4 to 1.2x10-3 mm3/Nm as the sliding distance is extended. The rate of wear for the AlP1 sample also changes, going from 2.37x10-4 to 1.03x10-3 mm3/Nm. The AlP5 coating sample also shows a surge in wear rate, going from 2.17x10-4 to 9.82x10-4 mm3/Nm. When compared to an uncoated brass pin, a pin coated with TiAlN wears down more slowly.

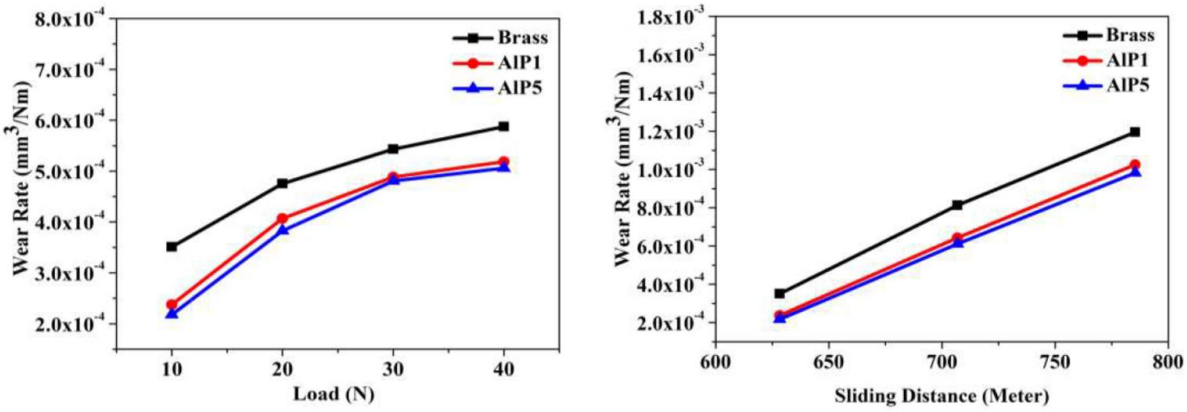

Figure 6. Wear rates of TiAlN-coated (at various pressure 1 and 5 Pa) and untreated brass pins at various (a) loads and (b) sliding distances.

Figures 7(a) and 7(b) show the effects of load and sliding distance on the wear rate of untreated and TiAlN coated brass pins produced at power of 275 and 450 W, respectively. Clearly, TiAlN-coated brass pins have a lower wear rate than their uncoated counterparts. Untreated and treated

 doi:10.20944/preprints202605.1513.v1

brass pins with TiAlN show wear rates between 1.83x10^{-4} and 5.87x10^{-4} mm^3/Nm when deposited at different powers on Al-Ti275 and AlTi450 samples. Factors such as sliding distance and applied load determine this range. When the load is raised from 10 to 40 N, the wear rate of untreated brass pins goes up from 3.51x10^{-4} to 5.87x10^{-4} mm^3/Nm. Similarly, the wear rate increases from 2.05x10^{-4} to 5.05x10^{-4} mm^3/Nm for the TiAlN coated brass pins sample. Similarly, the wear rate increases from 1.83x10^{-4} to 4.96x10^{-4} mm^3/Nm for the sample of brass pins coated with AlTi275. Figure 7(b) shows that when the sliding distance increases, the wear rate of the uncoated brass pin goes from 3.51x10^{-4} to 1.2x10^{-3} mm^3/Nm. Likewise, the AlTi275 coated brass pin sample has an increase in wear rate from 1.83x10^{-4} to 9.38x10^{-4} mm^3/Nm, while AlTi450 sample experiences an increase from 2.05x10^{-4} to 9.85x10^{-4} mm^3/Nm. The increase in the wear rate with sliding distance could be due to abrasive wear, where higher frictional heating inhibits abrasion. It is reported that as sliding speed increases, the wear rate of coating also increases.

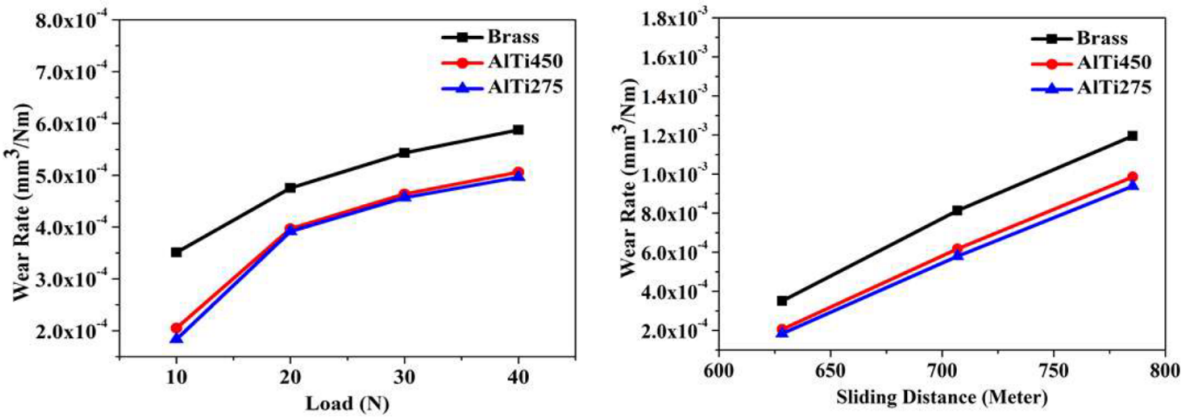

Figure 7. Wear rates of TiAlN-coated (at various aluminum power 450 and 275 W) and untreated brass pins at various (a) loads and (b) sliding distances.

The comparative analysis of wear rate reduction percentages for ternary coatings with different parameters is presented in Table 1. The AlTi275 coating exhibited the highest percentage decrease in wear rate among the TiAlN coatings, whereas the AlP1 coating demonstrated the lowest percentage reduction in wear rate among the TiAlN coatings. Table 2 presents a comparative analysis of the percentage reduction in coefficient of friction (COF) for ternary coatings across different parameters. The AlTi275 coating exhibited the highest percentage decrease in COF compared to the other TiAlN coatings, while the AlP1 coating had the lowest percentage reduction in COF.

Table 1. Comparing the effects of different factors on the wear reduction rate of ternary coatings.

Parameters	Sample Name	Reduction in Wear Rate (%)
Load (40 N)	AlP1	11.75
	AlP5	13.79
Sliding Distance (785 m)	AlP1	14.16
	AlP5	18.16
Load (40 N)	AlTi450	13.79
	AlTi275	15.50
Sliding Distance (785 m)	AlTi450	17.83
	AlTi275	21.75

The interdependence of hardness and grain size is well-known in classical deformation theory with regard to microstructural effects; this is shown by the Hall-Petch equation, which states that, given a grain size d, one may compute hardness using Equation (5)

$$H_d = H_0 + k_1 d^{-1/2} \quad (5)$$

 doi:10.20944/preprints202605.1513.v1

k_1 is a constant that is connected to the shear modulus (and thus E) and the critical shear stress for dislocation movement in the material, whereas H_0 is an intrinsic material property. The yield stress, which is a function of grain size ($\sigma_y = \sigma_0 + k_2\, d^{-1/2}$), also tends to rise linearly with respect to $d^{-1/2}$. Reducing material grain size improves tribological characteristics and makes materials harder [33].

Table 2. Comparing the effects of different factors on the coefficient of friction of ternary coatings.

Parameters	Sample Name	Reduction in COF (%)
Load (40 N)	AlP1	6.81
	AlP5	11.36
Sliding Distance (785 m)	AlP1	12.77
	AlP5	17.44
Load (40 N)	AlTi450	10.45
	AlTi275	13.63
Sliding Distance (785 m)	AlTi450	19
	AlTi275	23.67

4. Conclusions

Reactive DC magnetron sputtering was used for developing films of titanium aluminum nitride over brass substrates. Titanium power rates were fine-tuned and operational pressure was adjusted to accomplish the purpose. As the pressure was varied from 1 to 5 Pa, the X-ray diffraction (XRD) patterns revealed that TiAlN coatings had (103) and (107) structural orientations. Nevertheless, when modifying the titanium power levels, the peaks corresponding to (100), (103), and (107) were seen. The investigation demonstrated a distinct association between the rate of wear and the coefficient of friction, as well as the variations in operating pressure and power levels. The TiAlN-coated brass pins exhibit a variety of friction coefficients, specifically ranging from 0.195 to 0.24, in response to changes in pressure. However, when power levels are changed, the friction coefficient at room temperature varies between 0.19 and 0.23. The load and the sliding distance determine this variance. When exposed to the same conditions, the rate at which uncoated brass wears is higher than that of TiAlN coatings. The wear rates of TiAlN coating and brass vary between 1.03×10^{-3} and 5.87×10^{-4} mm^3/Nm. These rates depend on elements such as load, sliding distance, pressure, and titanium power.

Author Contributions: K.C.: Formal analysis, investigation, data curation, writing—original draft preparation. S.R: Conceptualization, methodology, software, validation, supervision. N.P.: Resources, writing—review and editing, data curation. DS: methodology, software, resources. V.V.: Methodology, Validation, Formal analysis, all authors have read and agreed to the published version of the manuscript.

Funding: This research received no external funding.

Institutional Review Board Statement: Not applicable.

Informed Consent Statement: Not applicable.

Data Availability Statement: Not applicable.

Conflicts of Interest: The authors declare no conflict of interest.

References

1. Patel, N.P.; Chauhan, K. V. Impact of Deposition Time and Working Pressure on Delay of Ice Formation on Aluminum Doped Zinc Oxide Thin Films. *Thin Solid Films* **2023**, *769*, 139750, doi:10.1016/j.tsf.2023.139750.
2. N. Gao, Z. Zhang, J. Deng, X. Guo, B. Cheng, H. Hou, Acoustic metamaterials for noise reduction: a review, Adv. Mater. Technol. 7 (6) (2022), 2100698

 doi:10.20944/preprints202605.1513.v1

3. Zhu, Q.; Hui, M.; Jin, P.; Joo, J.; Lee, C.; Le, K.; Chin, O.; Wang, S.; Kai, D.; Ji, R.; et al. Recent Advances in Nanotechnology-Based Functional Coatings for the Built Environment. *Mater Today Adv* **2022**, *15*, 100270, doi:10.1016/j.mtadv.2022.100270.
4. Nassef, M.G.A.; Nassef, B.G.; Hassan, H.S.; Nassef, G.A.; Elkady, M.; Pape, F. Tribological and Chemical–Physical Behavior of a Novel Palm Grease Blended with Zinc Oxide and Reduced Graphene Oxide Nano-Additives. Lubricants 2024, 12, 191. https://doi.org/10.3390/ lubricants12060191
5. Huang, L.; Li, L.; Zhao, Y.; Liu, Y.; Zheng, H.; Du, Z.; Liu, J.; Huang, L.; Li, L.; Zhao, Y.; et al. Citation: Microstructure and Properties of Ti6Al4V Surface Processed by Continuous Wave Laser in Different Atmospheres. **2024**, doi:10.3390/coatings.
6. Dang, M.N.; Singh, S.; King, H.J.; Navarro-Devia, J.H.; Le, H.; Pattison, T.G.; Hocking, R.K.; Wade, S.A.; Stephens, G.; Papageorgiou, A.; et al. Surface Enhancement of Titanium-Based Coatings on Commercial Hard Steel Cutting Tools. *Crystals (Basel)* **2024**, *14*, 470, doi:10.3390/cryst14050470.
7. Fan, J.; Xu, Y.X.; Geng, D.; Chen, L.; Wang, Q. Improving the Oxidation Resistance of TiAlN/CrAlO Coatings through CrAlON Interlayer. *Surf Coat Technol* **2024**, *479*, doi:10.1016/j.surfcoat.2024.130545.
8. Jeng, S.C. Oxidation Behavior and Microstructural Evolution of Hot-Dipped Aluminum Coating on Ti-6Al-4V Alloy at 800°C. *Surf Coat Technol* **2013**, *235*, 867–874, doi:10.1016/j.surfcoat.2013.09.023.
9. Yan, N.; Zhu, Z.; Cheng, Y.; Liu, F.; Shen, M.; Li, H. Preparation and Performance of a Cr/CrN/TiAlCN Composite Coating on a GCr15 Bearing Steel Surface. *Coatings* **2024**, *14*, 782, doi:10.3390/coatings14070782.
10. Ben Hassine, M.; Andrén, H.O.; Iyer, A.H.S.; Lotsari, A.; Bäcke, O.; Stiens, D.; Janssen, W.; Manns, T.; Kümmel, J.; Halvarsson, M. Growth Model for High-Al Containing CVD TiAlN Coatings on Cemented Carbides Using Intermediate Layers of TiN. *Surf Coat Technol* **2021**, *421*, doi:10.1016/j.surfcoat.2021.127361.
11. Niu, X.; Du, Y.; Liu, J.; Li, J.; Sun, J.; Guo, Y. Facile Synthesis of TiO2/MoS2 Composites with Co-Exposed High-Energy Facets for Enhanced Photocatalytic Performance. *Micromachines (Basel)* **2022**, *13*, doi:10.3390/mi13111812.
12. Wilczek, A.; Morgiel, J.; Rogal, L.; Wojciech, M.; Smolik, J. Microstructure AndWear of (CrN/CrAlN)/(CrAlN/VN) and (CrN/TiAlN)/(TiAlN/VN) Coatings for Molds Used in High Pressure Casting of Aluminum. *Coatings* **1967**, *10*, doi:10.3390/coatings10030261.
13. Zeng, Q. Thermal Stability and High-Temperature Super Low Friction of γ-Fe2O3@SiO2 Nanocomposite Coatings on Steel. Lubricants 2024, 12, 223. https://doi.org/10.3390/lubricants 12060223
14. Sandu, C.S.; Sanjinés, R.; Benkahoul, M.; Medjani, F.; Lévy, F. Formation of Composite Ternary Nitride Thin Films by Magnetron Sputtering Co-Deposition. *Surf Coat Technol* **2006**, *201*, 4083–4089, doi:10.1016/j.surfcoat.2006.08.100.
15. Deng, B.; Tao, Y.; Guo, D. Effects of Vanadium Ion Implantation on Microstructure, Mechanical and Tribological Properties of TiN Coatings. *Appl Surf Sci* **2012**, *258*, 9080–9086, doi:10.1016/j.apsusc.2012.06.001.
16. Gao, B.; Du, X.; Li, Y.; Wei, S.; Zhu, X.; Song, Z. Effect of Deposition Temperature on Hydrophobic CrN/AlTiN Nanolaminate Composites Deposited by Multi-Arc-Ion Plating. *J Alloys Compd* **2019**, *797*, 1–9, doi:10.1016/j.jallcom.2019.05.069.
17. Ma, H.; Miao, Q.; Zhang, G.; Liang, W.; Wang, Y.; Sun, Z.; Lin, H. The Influence of Multilayer Structure on Mechanical Behavior of TiN/TiAlSiN Multilayer Coating. *Ceram Int* **2021**, *47*, 12583–12591, doi:10.1016/j.ceramint.2021.01.117.
18. Liu, Z.R.; Chen, L.; Du, Y.; Zhang, S. Influence of Ru-Addition on Thermal Decomposition and Oxidation Resistance of TiAlN Coatings. *Surf Coat Technol* **2020**, *401*, doi:10.1016/j.surfcoat.2020.126234.
19. Ghufran, M.; Uddin, G.M.; Arafat, S.M.; Jawad, M.; Rehman, A. Development and Tribo-Mechanical Properties of Functional Ternary Nitride Coatings: Applications-Based Comprehensive Review. *Proceedings of the Institution of Mechanical Engineers, Part J: Journal of Engineering Tribology* 2021, *235*, 196–232.
20. Walczak, M.; Pasierbiewicz, K.; Szala, M. Adhesion and Mechanical Properties of TiAlN and Altin Magnetron Sputtered Coatings Deposited on the DMSL Titanium Alloy Substrate. In Proceedings of the Acta Physica Polonica A; Polish Academy of Sciences, 2019; Vol. 136, pp. 294–298.
21. Pana, I.; Braic, V.; Dinu, M.; Massima Mouele, E.S.; Parau, A.C.; Petrik, L.F.; Braic, M. In Vitro Corrosion of Titanium Nitride and Oxynitride-Based Biocompatible Coatings Deposited on Stainless Steel. *Coatings* **2020**, *10*, doi:10.3390/COATINGS10080710.

 doi:10.20944/preprints202605.1513.v1

22. Bahi, R.; Nouveau, C.; Beliardouh, N.E.; Ramoul, C.E.; Meddah, S.; Ghelloudj, O. Surface Performances of Ti-6Al-4V Substrates Coated PVD Multilayered Films in Biological Environments. *Surf Coat Technol* **2020**, *385*, doi:10.1016/j.surfcoat.2020.125412.
23. Patnaik, L.; Maity, S.R.; Kumar, S. Lubricated Sliding of CFRPEEK/AlCrN Film Tribo-Pair and Its Effect on the Mechanical Properties and Structural Integrity of the AlCrN Film. *Mater Chem Phys* **2021**, *273*, doi:10.1016/j.matchemphys.2021.124980.
24. Natrayan, L.; Balaji, S.; Bharathiraja, G.; Kaliappan, S.; Veeman, D.; Mammo, W.D. Experimental Investigation on Mechanical Properties of TiAlN Thin Films Deposited by RF Magnetron Sputtering. *J Nanomater* **2021**, *2021*, doi:10.1155/2021/5943486.
25. Radhika Ramadoss, N. Kumar, R. Pandian, S. Dash, T.R. Ravindran, D. Arivuoli, A.K. Tyagi, Tribological properties and deformation mechanism of TiAlN coating sliding with various counterbodies, *Tribology International*, Volume 66, 2013, Pages 143-149.
26. Ait-Djafer, A.Z.; Saoula, N.; Aknouche, H.; Guedouar, B.; Madaoui, N. Deposition and Characterization of Titanium Aluminum Nitride Coatings Prepared by RF Magnetron Sputtering. In Proceedings of the Applied Surface Science; Elsevier B.V., September 30 2015; Vol. 350, pp. 6–9.
27. Patel, N.P.; Chauhan, K. V; Desai, M.K. Effects of Power and Temperature on the Structural , Anti-Icing , Wettability , and Optical Properties of Zinc Oxide Thin Films. *Ceram Int* **2023**, doi:10.1016/j.ceramint.2023.05.233.
28. X. Wang, C.H. Zhang, X. Cui, S. Zhang, J. Chen, J.B. Zhang, Novel gradient alloy steel with quasi-continuous ratios fabricated by SLM: material microstructure and wear mechanism, Mater. Char. 174 (2021), 111020, https://doi.org/10.1016/j. matchar.2021.111020.
29. Bobzin, K.; Lugscheider, E.; Maes, M.; Immich, P.; Bolz, S. Grain Size Evaluation of Pulsed TiAlN Nanocomposite Coatings for Cutting Tools. *Thin Solid Films* **2007**, *515*, 3681–3684, doi:10.1016/j.tsf.2006.11.002.
30. Chen, Z.; Gui, N.; Sun, Y.; Yang, X.; Tu, J.; Jiang, S. Experimental Study of Friction Coefficient of Graphite for High-Temperature Gas-Cooled Reactors. *Nuclear Engineering and Design* **2024**, *423*, doi:10.1016/j.nucengdes.2024.113162.
31. Menezes, P.; Sundeep, I.; Nosonovsky, M.; Kailas, S.; Lovell, M. *Tribology for Scientists and Engineers*; 2013; ISBN 978-1-4614-1944-0.
32. Chauhan, K. V.; Rawal, S.; Patel, N.P.; Subhedar, D.G. Impact of Deposition Power and Gas Flow Ratio on the Tribological Properties of Titanium Vanadium Nitride Thin Films. *Micromachines (Basel)* **2023**, *14*, doi:10.3390/mi14091788.
33. Tsui, T. Y., G. M. Pharr, W. C. Oliver, C. S. Bhatia, R. L. White, S. Anders, A. Anders, and I. G. Brown. 1995. "Nanoindentation and Nanoscratching of Hard Carbon Coatings for Magnetic Disks." MRS Proceedings 383: 447.